ORIGINAL ARTICLE

A SIMPLE AND LOW-COST METHOD FOR FABRICATION OF NON-PLANAR PDMS MICROFLUIDIC CHANNEL

Tuan Ngoc Anh Vo [1,3]*, Anh Son Tran [1,3], and Trung Nghia Tran [2,3]

[1] *Faculty of Mechanical Engineering, Ho Chi Minh University of Technology (HCMUT), 268 Ly Thuong Kiet Street, Dien Hong Ward, Ho Chi Minh City, VIETNAM*

[2] *Laboratory of Laser Technology, Faculty of Applied Science, Ho Chi Minh University of Technology (HCMUT), 268 Ly Thuong Kiet Street, Dien Hong Ward, Ho Chi Minh City, VIETNAM*

[3] *Vietnam National University Ho Chi Minh City (VNU-HCM), Linh Xuan Ward, Ho Chi Minh City, VIETNAM*

(**Received** 6 December 2025, **Revised** 13 December 2025, **Accepted** 17 December 2025)

*Corresponding author: vnatuan@hcmut.edu.vn

DOI: 10.5875/35wp8n53

Abstract: This research introduces a micromilling-based method for fabricating prototypes of poly(methyl methacrylate) (PMMA). This approach enables rapid prototyping of non-planar polydimethylsiloxane (PDMS) microfluidic channels, which are difficult to fabricate using traditional soft lithography methods. To achieve high fidelity, we improve the surface quality of the PMMA molds by systematically optimizing key machining parameters, including spindle speed, feed rate, and cutting depth. These optimized conditions are subsequently applied to CNC machining of complex three-dimensional curved geometries. Using a partial-curing method, the resulting PDMS devices achieve robust bonding strengths of up to 184 kPa without plasma treatment or specialized apparatus. This method offers a cost-efficient and accessible alternative for fabricating intricate non-planar microfluidic systems, markedly enhancing the design versatility and application prospects of PDMS-based platforms.

Keywords: Micro-milling; Non-planar microchannel; PDMS.

Introduction

Microfluidic technology has rapidly emerged as one of the most influential platforms in modern science and engineering. Microfluidic chips, also referred to as lab-on-a-chip systems, integrate a network of microscale channels that are capable of manipulating small volumes of fluids with high precision. These devices mimic laboratory processes on a miniature scale, allowing chemical reactions [1], separations [2], and biological assays [3] to be conducted with minimal reagent consumption and shortened analysis times. The advantages of microfluidics include reduced sample and reagent use, faster reaction kinetics, enhanced portability, and the possibility of high-throughput parallel analysis. Because of these benefits, microfluidic chips have found applications across diverse fields such as biomedical diagnostics, point-of-care testing, drug screening, single-cell analysis, environmental monitoring, and chemical synthesis[4-6]. For instance, microfluidic devices are increasingly employed for early disease biomarker detection, enabling sensitive and rapid assays that can be performed outside of centralized laboratories. Similarly, microfluidic cell culture platforms provide physiologically relevant environments for studying cellular behavior, tissue engineering, and organ-on-chip models[7, 8]. The breadth of these applications underscores the critical importance of developing robust, flexible, and cost-effective fabrication methods for microfluidic systems.

The fabrication of microfluidic chips has traditionally relied on cleanroom-based microfabrication processes. Among these, soft lithography using SU-8 photoresist remains one of the most widely adopted methods [9]. In this approach, SU-8 is patterned onto a silicon wafer by photolithography to create a mold, which is then used for casting poly(dimethylsiloxane) (PDMS). SU-8 lithography provides high resolution, excellent reproducibility, and compatibility with planar channel designs, making it suitable for many applications in microfluidics [10]. However, the method has significant limitations. It requires access to cleanroom facilities, photomasks, and UV lithography equipment, which are

costly and time-consuming. Moreover, SU-8 molds are typically restricted to planar geometries, limiting the ability to fabricate three-dimensional or curved structures[11]. To overcome these challenges, alternative approaches have been explored, including 3D printing technologies such as Fused deposition modeling (FDM)[12], Stereolithography (SLA)[13] and Digital light processing (DLP) [14]. These additive manufacturing methods allow direct fabrication of molds or even complete microfluidic devices. While 3D printing offers rapid prototyping and design flexibility, it often suffers from limited resolution, surface roughness, and incomplete replication of fine features, especially at the microscale[15]. Thus, despite their advantages, both SU-8 lithography and 3D printing present drawbacks that restrict their applicability for fabricating advanced microfluidic devices.

In recent years, computer numerical control (CNC) micromilling has gained attention as a promising alternative for fabricating molds used in PDMS microfluidics. CNC milling provides a maskless, rapid, and cost-effective process in which digital designs are directly translated into physical molds on polymer substrates such as polymethyl methacrylate (PMMA)[16, 17]. Unlike photolithography, CNC milling does not require specialized facilities, making it accessible to laboratories without cleanroom infrastructure. The process is versatile, allowing researchers to rapidly iterate and modify channel designs by simply adjusting CAD models. Additionally, CNC milling produces smooth surfaces and precise geometries when optimized parameters are employed, resulting in PDMS devices with reliable performance. Compared with 3D printing, CNC milling often achieves higher dimensional accuracy and better surface quality, both of which are essential for fluidic control and optical imaging in microfluidic applications [18, 19]. These advantages have led to a growing adoption of CNC micromilling as a prototyping method for microfluidic mold fabrication.

Within CNC milling, the most commonly used tool has been the flat end-mill. End-mill tools are suitable for machining two-dimensional channel networks with uniform depths and sharp edges, making them well suited for planar microfluidics. However, their flat geometry imposes inherent limitations. Specifically, end-mills are not capable of efficiently producing smooth curved surfaces, rounded cavities, or channels with variable depths[20, 21]. These types of non-planar geometries are increasingly relevant in advanced microfluidics, where channel cross-sectional shape can significantly influence fluid dynamics, mixing efficiency, and biological compatibility[22, 23]. To address these challenges, the use of ball-end milling tools has emerged as a powerful approach. A ball-end mill, characterized by its hemispherical cutting tip, enables the fabrication of three-dimensional and contoured features. By distributing cutting forces along its curved tip, the ball-end mill is particularly effective for generating sloped surfaces, rounded grooves, and hemispherical wells with reduced surface roughness. This capability opens up new design opportunities in microfluidics, allowing for novel device functionalities such as improved mixing, droplet control, and cell trapping within curved microchambers.

The present study builds upon this capability by exploring the use of ball-end CNC milling for the fabrication of PMMA molds for PDMS casting. While flat end-mill micromilling has been reported previously, systematic investigations of ball-end milling for microfluidic mold preparation remain limited. The novelty of this research lies in two key aspects. First, by employing ball-end milling, we demonstrate the fabrication of non-planar microfluidic features that cannot be easily achieved with either SU-8 lithography or flat end-milling. This includes hemispherical cavities, sloped channels, and smoothly curved grooves, which enhance device functionality. Second, we incorporate a simplified bonding strategy based on partial curing of PDMS layers, eliminating the need for plasma treatment or expensive bonding equipment[24, 25]. This combination results in a cost-effective, accessible, and versatile approach to fabricating advanced PDMS microfluidic devices. By expanding the design space beyond planar structures, this method significantly increases the flexibility and application potential of microfluidic technology in biomedical, chemical, and environmental applications.

Tuan Ngoc Anh Vo He is a lecturer in the Faculty of Mechanical Engineering, Ho Chi Minh City University of Technology (HCMUT). His research topic is the fabrication of microfluidic devices, microfabrication technique, and relative applications

Anh Son Tran He is a professor in the Faculty of Mechanical Engineering, Ho Chi Minh City University of Technology (HCMUT). His research topic is injection molding, advanced fabrication technology.

Trung Nghia Tran He is currently a professor with HCMUT. His current research interests include biomedical instruments, biomedical optics, bioimpedance, electrical impedance tomography, trans-illumination imaging, and photobiomodulation. He is a member of SPIE and OSA.

Materials and methods

Materials

The materials employed in this study included polymethyl methacrylate (PMMA, CHIMEI, Taiwan) as the primary substrate for micromilling experiments, polydimethylsiloxane (PDMS, Sylgard 184, Dow Corning, USA) for soft lithography and device replication, Epoxy

Glue (AB Glue, Taiwan) for sealing of tubing into the microchip. Micromilling was performed using micro end mills (NS TOOL Co., Ltd., Japan), which provided the precision necessary for fabricating microchannels on PMMA substrates.

Fabrication testing sample

A test sample was fabricated on a PMMA substrate with a thickness of 4 mm to evaluate the effects of ball-end milling parameters on the surface gloss of the mold. The testing model was designed using NX software, as shown in Figure 1(a). The toolpath on the exterior contour was generated for machining with a 2 mm end-mill tool, as show in Figure 1(b), while the main surface was machined using a 1 mm ball-end mill. Table 1 presents the ball-end mill tool parameters, the toolpath strategy, and the machining conditions, including air blowing for chip removal without liquid coolant.

Table 1. Ball-end mill specifications, toolpath strategy, and machining conditions.

Parameter	Value
Type	Ball-end mill
Material	Carbide Micro Grain
Diameter	Radius-0.5 mm
Stepover	0.1mm
Cut pattern	Zig Zag
Drive Method	Surface Area
Cooling	Air

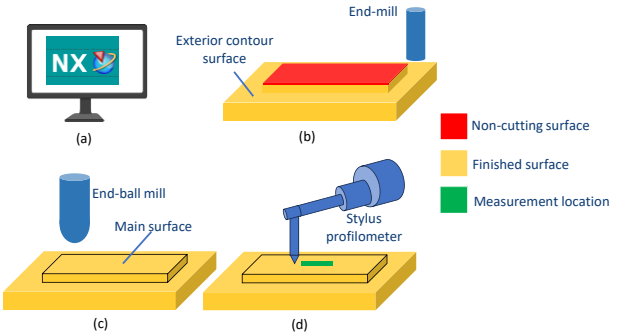

Figure 1. Design and fabrication of the test sample: (a) Design the sample using NX software, (b) 3D testing model, (c) Fabrication testing model by ball-end milling tool, and (d) Stylus profilemeter setup.

A rough-milling pass is subsequently performed to remove a 1-mm layer from the residual surface, ensuring an adequate machining allowance for the finishing phase. A 1-mm-diameter ball-end mill is employed to manufacture the primary surface, with a cutting depth of 10-30 µm (Figure 1(c)). Next, the cutting conditions were varied, as shown in Table 2, to investigate the parameters affecting the surface quality of PMMA when using a ball-end mill. The factors considered in this study included spindle speed, feed rate, and depth of cut.

Figure 1(d) shows the platform and the stylus profilometer (Handysurf+, Accretech, Japan) used to evaluate the surface roughness of the micromilled PMMA substrates machined by the ball-end mill. The measurements were performed at the center region of the chip, with a measurement length of approximately 2 mm. Figures 2(b)–2(d) illustrate the machined samples produced under the cutting conditions listed in Table 2.

The workpiece material depicted in Figure 2(a) has dimensions of 40 × 65 mm. The cutting experiments were conducted using a micro-milling machine (VF-2, Haas, USA), specifically designed for the fabrication of microfluidic chips.

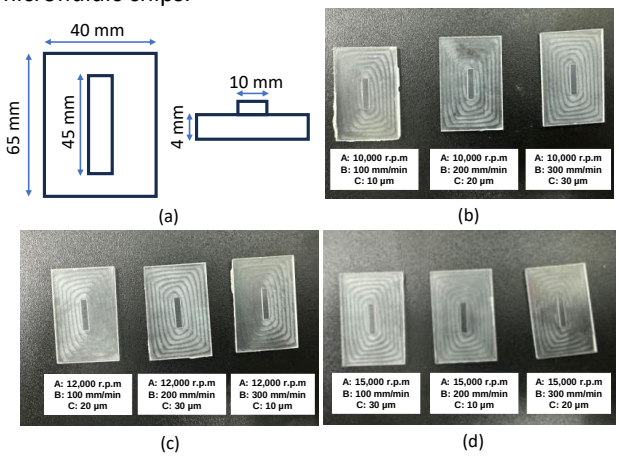

Figure 2. (a) Dimensions of the testing sample, (b)~(d) Images of the test sample with various conditions.

Table 2. Experimental results based on various factors and levels

No.	(A)-Spindle speed (r.p.m)	(B)-Feedrate (mm/min)	(C)- DOC (µm)	Ra (µm)
1	10,000	100	10	0.42
2	10,000	200	20	0.69
3	10,000	300	30	0.35
4	12,000	100	20	0.21
5	12,000	200	30	0.27
6	12,000	300	10	0.29
7	15,000	100	30	0.41
8	15,000	200	10	0.31
9	15,000	300	20	0.34

Fabrication non-planar and bonding microchip

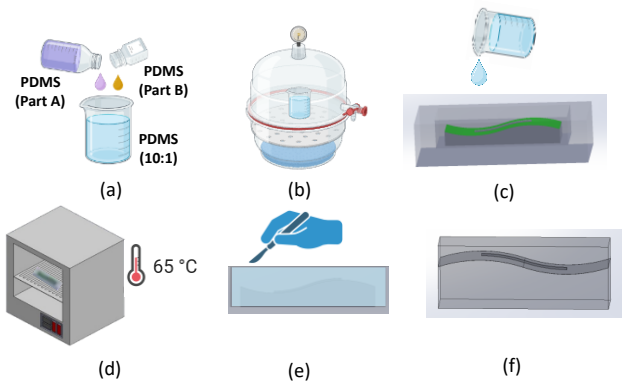

Figure 3. Schematic of casting PDMS into the mold by (a) Pouring the premixed PDMS, (b) Degassing the PDMS poured in the mold to remove trapped air, (c) Pouring of the mixture of PDMS into the master PMMA mold, (d) Curing it in the oven at 65°C, (e) PDMS peeling off the mold, and (f) Fully non-planar PDMS chip.

After determining the optimal cutting parameters for achieving the desired surface finish on PMMA with a ball-end mill, these parameters were subsequently used to produce the mold set for casting the non-planar PDMS microfluidic chip. The upper and lower mold parts were engineered in accordance with the specifications described in the previous section. In this study, a partial-curing bonding method was utilized to assemble the PDMS microfluidic device.

To prepare the PDMS material, the elastomer base and curing agent were thoroughly mixed manually for 10 minutes in a 10:1 ratio, as illustrated in Figure 3(a). The mixture was subsequently placed in a vacuum chamber for approximately 15 minutes to eliminate the contained air bubbles, as depicted in Figure 3(b). Following degassing, the liquid PDMS was transferred into the molds for curing, as illustrated in Figure 3(c). Partial-curing durations ranging from 45 to 85 minutes were tested at 65 °C in the oven, as shown in Figure 3(d). Once the PDMS attained a semi-solid state, the molded halves were carefully detached from the molds employing a precision knife, as illustrated in Figure 3(e).

Subsequently, two inlet/outlet openings were formed in the upper section utilizing a circular tool to facilitate tubing connections. Finally, the upper and lower PDMS halves were precisely aligned and cured overnight at 65°C to form a fully bonded, operational non-planar microfluidic chip, as illustrated in Figure 3(f).

Results and discussion

Experiment results

Table 2 illustrates a representative outcome obtained from a series of nine investigations. All measured average surface roughness values range from 0.21 µm to over 0.69 µm.

Factor analysis was conducted to identify the parameters with the strongest and weakest influences on the surface roughness of the PMMA mold. Table 1 presents the signal-to-noise (S/N) ratios obtained from the three measurement samples. Because lower surface roughness is desired, the signal-to-noise ratio was calculated using the "Smaller-is-better'' criterion according to Eq. (1), where n = 3 represents the number of repeated measurements for each parameter combination, and y_i^2 denotes the squared surface roughness value for each measurement.

$$S/N = -10\log_{10}\left(\frac{1}{n}\sum_{i=1}^{n} y_i^2\right) \quad (1)$$

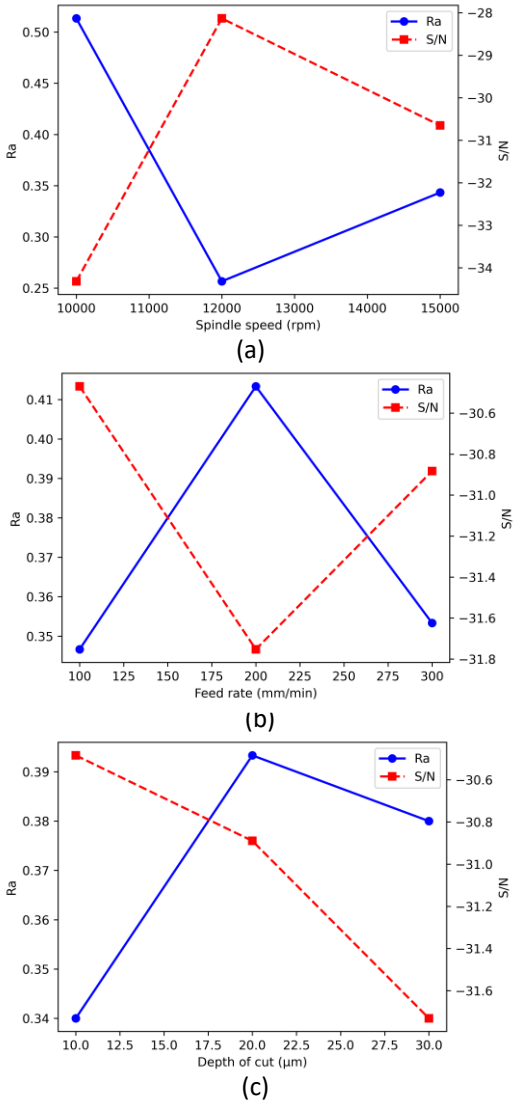

Figure 4. S/N ratios and surface roughness corresponding to three main factors and three levels: (a) Spindle speed, (b) Feed rate, and (c) Depth of cut.

Factor analysis

Figure 4(a)~(c) plots the average S/N ratios listed in Table 2 and the corresponding average surface roughness. The signal-to-noise (S/N) response analysis indicated significant variations in the impact of machining parameters on surface irregularity. In Table 3, Spindle speed (Factor A) demonstrated the greatest range (5.230), suggesting it was the primary factor influencing the machining response. The observed sensitivity implies that fluctuations in cutting speed significantly influenced crystal formation and tool-material interaction, thereby resulting in discernible alterations in surface finish. Feed rate (Factor B) exhibited a moderate influence, spanning a range of 1.390. Conversely, depth of cut (Factor C) yielded the narrowest range (0.720), suggesting a minimal impact among the examined micromilling parameters. Based on the level-average signal-to-noise (S/N) ratio trends, the optimal parameters for minimizing surface roughness were determined to be spindle speed (12,000 r.p.m), feed rate (100 mm/min), depth of cut (10 µm).

Table 3 Factor to analysis cutting parameter

Level	(A)-Spindle speed (r.p.m)	(B)-Feed rate (mm/min)	(C)-DOC (µm)
1	6.533	9.480	9.350
2	11.763	8.230	8.630
3	9.033	9.620	9.350
Max	11.763	9.620	9.350
Min	6.533	8.230	8.630
Range	5.230	1.390	0.720
Rank	1	2	3

Experiment Results: Non-planar PDMS

We performed burst-pressure experiments to evaluate the bonding strength of the non-planar microfluidics chip fabricated via the partial-curing technique. Figure 5(a) shows the schematic diagram of the testing system, while Figure 5(b) depicts the actual testing setup. Bonding strength was evaluated utilizing a fluidic system comprising a syringe pump for injecting red food dye, a pressure meter (PS-9303SD, Lutron Electronic Enterprise Co., Ltd., Taiwan), and a pressure sensor (PS100-20 bar, Yalab, Taiwan) connected to the pressure meter.

Bonding strength is defined as the stress at which the camera detects interfacial separation. This testing approach is particularly appropriate for applications that demand extended chip durability and consistent stability.

The bonding efficacy of PDMS under different partial-curing conditions is depicted in Figure 6. At 65 °C for 45 minutes, the PDMS mixture remained undercrosslinked, allowing the replica to be readily removed from the mold due to the incompletely formed microchannel structure. Conversely, at 85 minutes, partial curing was no longer attainable as the PDMS surface had already undergone complete crosslinking, thereby inhibiting successful bonding. As illustrated in Figure 6, the maximum bonding strength was achieved at 65 minutes of curing, suggesting that this time interval is optimal for microchannel replication while maintaining robust interlayer adhesion.

From these results, we can conclude the following: (1) PMMA molds fabricated by micromachining are well suited for replicating PDMS structures with non-planar or three-dimensional curved geometries, demonstrating that the mold design can reliably preserve complex surface features during casting, (2) The proposed PDMS bonding approach enables the assembly of 3D microfluidic chips without the need for expensive equipment such as plasma systems or silane-based surface treatments. Instead, a simple partial-curing strategy provides sufficient interlayer adhesion, offering a low-cost and accessible method for fabricating multilayer PDMS microfluidic devices.

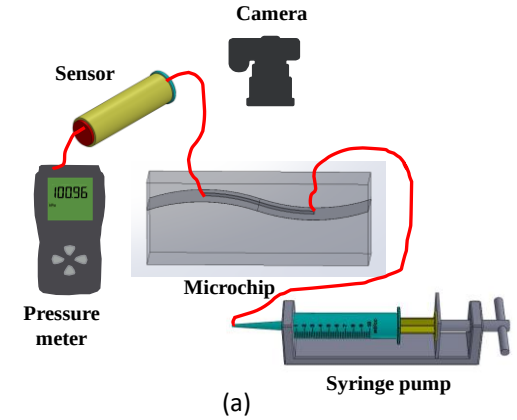

(a)

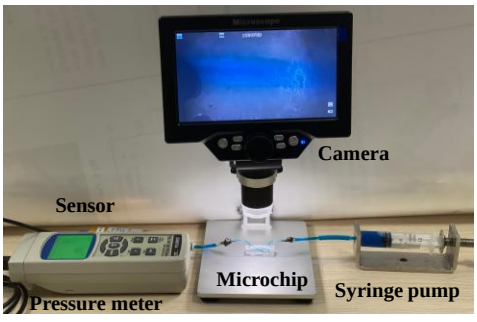

(b)

Figure 5. (a) System used to test the bonding strength of bonded microfluidic chips, including a camera, , a pressure meter, a manual syringe pump with a pressure sensor, and (b) Experiment setup.

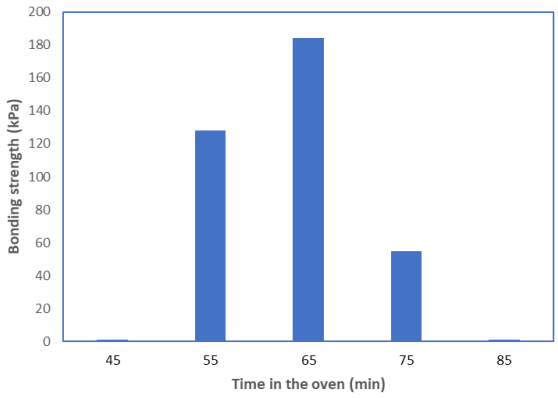

Figure 6. The bonding strength of the PDMS chip as a function of the partial-curing time at 65 °C

Conclusion

This study provides the first systematic demonstration of ball-end milling for fabricating PMMA molds with complex, non-planar geometries for PDMS microfluidic fabrication. By optimizing the machining parameters, the smoothest surfaces—suitable for high-fidelity PDMS replication and strong interlayer bonding—were achieved at a spindle speed of 12,000 r.p.m, feed rate of 100 mm/min, and depth of cut of 10 µm. Moreover, the work shows that non-planar PDMS microfluidic chips can be reliably assembled using a simple partial-curing bonding method, eliminating the need for plasma treatment or silane activation while still achieving bonding strengths above 180 kPa. These findings open the door to low-cost fabrication of curved or 3D microfluidic architectures, enabling future applications in micro-optics, organ-on-chip systems, and advanced droplet manipulation.

Acknowledgment

This research is funded by Vietnam National University Ho Chi Minh City (VNU-HCM) under grant number C2024-20-08. We acknowledge Ho Chi Minh City University of Technology (HCMUT), VNU-HCM, for supporting this study.

References

[1] M. Fani, P. Pourafshary, P. Mostaghimi, and N. Mosavat, "Application of microfluidics in chemical enhanced oil recovery: A review," *Fuel,* vol. 315, p. 123225, 2022.

[2] S. Lin *et al.*, "Progress in microfluidics-based exosome separation and detection technologies for diagnostic applications," *Small,* vol. 16, no. 9, p. 1903916, 2020.

[3] M. Adampourezare, G. Dehghan, M. Hasanzadeh, and M.-A. H. Feizi, "Application of lateral flow and microfluidic bio-assay and biosensing towards identification of DNA-methylation and cancer detection: recent progress and challenges in biomedicine," *Biomedicine & Pharmacotherapy,* vol. 141, p. 111845, 2021.

[4] C. M. Pandey *et al.*, "Microfluidics based point-of-care diagnostics," *Biotechnology journal,* vol. 13, no. 1, p. 1700047, 2018.

[5] M. Yew, Y. Ren, K. S. Koh, C. Sun, and C. Snape, "A review of state-of-the-art microfluidic technologies for environmental applications: Detection and remediation," *Global Challenges,* vol. 3, no. 1, p. 1800060, 2019.

[6] X. Liu, W. Zheng, and X. Jiang, "Cell-based assays on microfluidics for drug screening," *ACS sensors,* vol. 4, no. 6, pp. 1465-1475, 2019.

[7] T. Osaki, V. Sivathanu, and R. D. Kamm, "Vascularized microfluidic organ-chips for drug screening, disease models and tissue engineering," *Current opinion in biotechnology,* vol. 52, pp. 116-123, 2018.

[8] J. Dornhof, J. Kieninger, H. Muralidharan, J. Maurer, G. A. Urban, and A. Weltin, "Microfluidic organ-on-chip system for multi-analyte monitoring of metabolites in 3D cell cultures," *Lab on a Chip,* vol. 22, no. 2, pp. 225-239, 2022.

[9] G. M. Whitesides, E. Ostuni, S. Takayama, X. Jiang, and D. E. Ingber, "Soft lithography in biology and biochemistry," *Annual review of biomedical engineering,* vol. 3, no. 1, pp. 335-373, 2001.

[10] R. Martinez-Duarte and M. Madou, "SU-8 photolithography and its impact on microfluidics," *Microfluidics and nanofluidics handbook,* no. 2006, pp. 231-268, 2011.

[11] P. Abgrall, V. Conedera, H. Camon, A. M. Gue, and N. T. Nguyen, "SU-8 as a structural material for labs-on-chips and microelectromechanical systems," *Electrophoresis,* vol. 28, no. 24, pp. 4539-4551, 2007.

[12] Y. Hwang, O. H. Paydar, and R. N. Candler, "3D printed molds for non-planar PDMS microfluidic channels," *Sensors and Actuators A: Physical,* vol. 226, pp. 137-142, 2015.

[13] N. Bhattacharjee, C. Parra-Cabrera, Y. T. Kim, A. P. Kuo, and A. Folch, "Desktop-stereolithography 3D-printing of a poly (dimethylsiloxane)-based material with sylgard-184 properties," *Advanced materials,* vol. 30, no. 22, p. 1800001, 2018.

[14] D. H. Han, U. Oh, and J.-K. Park, "Characterization of PDMS microchannels using horizontally or vertically formed 3D-Printed molds by digital light projection," *ACS omega,* vol. 8, no. 21, pp. 19128-19136, 2023.

[15] S. Razavi Bazaz *et al.*, "Rapid softlithography using 3D-printed molds," *Advanced materials*

technologies, vol. 4, no. 10, p. 1900425, 2019.

[16] S. Qu, J. Zhao, and T. Wang, "Experimental study and machining parameter optimization in milling thin-walled plates based on NSGA-II," *The International Journal of Advanced Manufacturing Technology,* vol. 89, no. 5, pp. 2399-2409, 2017.

[17] E. Behroodi, H. Latifi, Z. Bagheri, E. Ermis, S. Roshani, and M. Salehi Moghaddam, "A combined 3D printing/CNC micro-milling method to fabricate a large-scale microfluidic device with the small size 3D architectures: An application for tumor spheroid production," *Scientific reports,* vol. 10, no. 1, p. 22171, 2020.

[18] A. K. Sen, A. Raj, U. Banerjee, and S. R. Iqbal, "Soft lithography, molding, and micromachining techniques for polymer micro devices," in *Microfluidic Electrophoresis: Methods and Protocols*: Springer, 2018, pp. 13-54.

[19] A. Javidanbardan, A. M. Azevedo, V. Chu, and J. P. Conde, "A systematic approach for developing 3D high-quality PDMS microfluidic chips based on micromilling technology," *Micromachines,* vol. 13, no. 1, p. 6, 2021.

[20] B. Xue, Y. Geng, Y. Yan, G. Ma, D. Wang, and Y. He, "Rapid prototyping of microfluidic chip with burr-free PMMA microchannel fabricated by revolving tip-based micro-cutting," *Journal of Materials Processing Technology,* vol. 277, p. 116468, 2020.

[21] D. J. Guckenberger, T. E. De Groot, A. M. Wan, D. J. Beebe, and E. W. Young, "Micromilling: a method for ultra-rapid prototyping of plastic microfluidic devices," *Lab on a Chip,* vol. 15, no. 11, pp. 2364-2378, 2015.

[22] L. Balasubramaniam, R. Arayanarakool, S. D. Marshall, B. Li, P. S. Lee, and P. C. Chen, "Impact of cross-sectional geometry on mixing performance of spiral microfluidic channels characterized by swirling strength of Dean-vortices," *Journal of Micromechanics and Microengineering,* vol. 27, no. 9, p. 095016, 2017.

[23] A. N. Cookson, D. J. Doorly, and S. J. Sherwin, "Efficiently generating mixing by combining differing small amplitude helical geometries," *Fluids,* vol. 4, no. 2, p. 59, 2019.

[24] A. Borók, K. Laboda, and A. Bonyár, "PDMS bonding technologies for microfluidic applications: A review," *Biosensors,* vol. 11, no. 8, p. 292, 2021.

[25] A. Ansari, R. Trehan, C. Watson, and S. Senyo, "Increasing silicone mold longevity: A review of surface modification techniques for PDMS-PDMS double casting," *Soft materials,* vol. 19, no. 4, pp. 388-399, 2021.

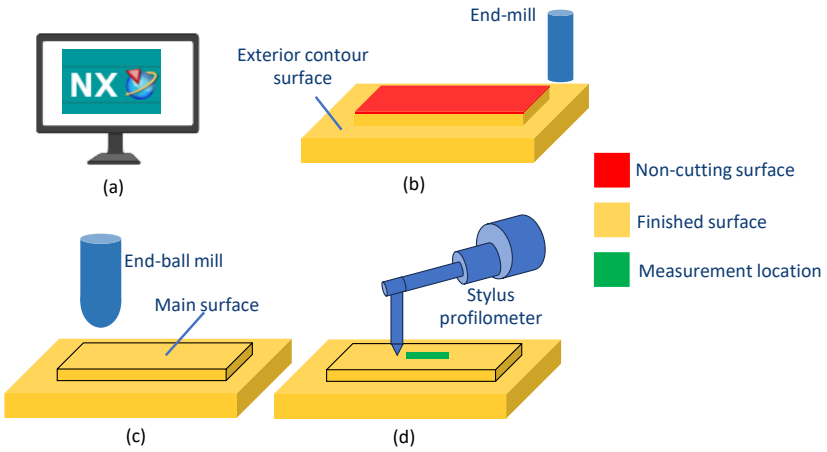

Figure 1. Design and fabrication of the test sample: (a) Design the sample using NX software, (b) 3D testing model, (c) Fabrication testing model by ball-end milling tool, and (d) Stylus profilemeter setup.

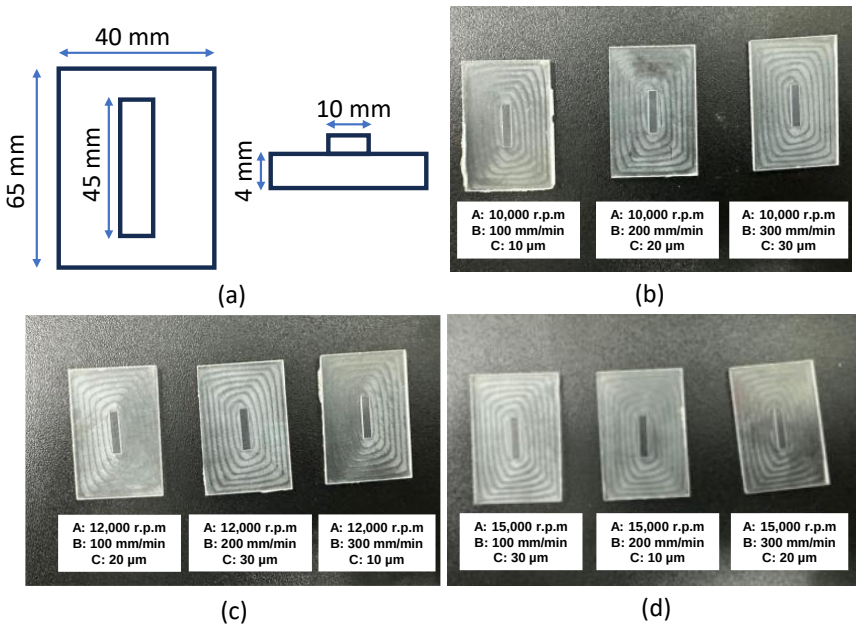

Figure 2. (a) Dimentional of the testing sample, (b)~(c) Images of the test sample with various conditions.

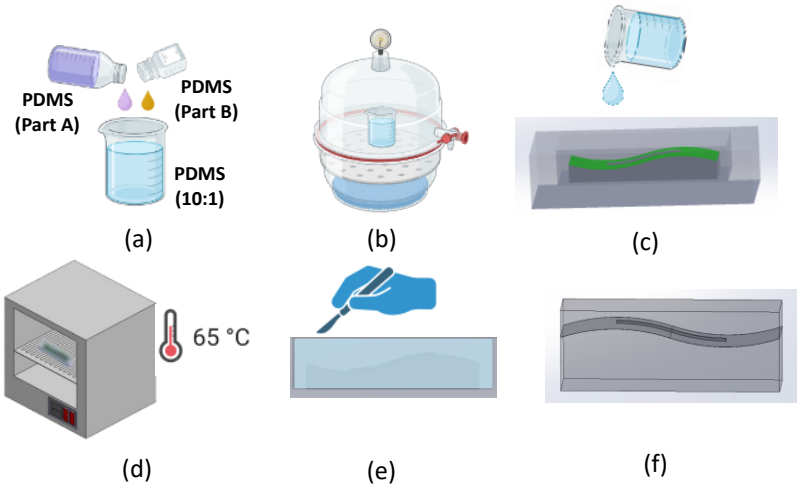

Figure 3. Schematic of casting PDMS into the mold by (a) pouring the premixed PDMS, (b) Degassing the PDMS poured in the mold to remove trapped air, (c) Pouring of the mixture of PDMS into the master PMMA mold, (d) curing it in the oven at 65°C, (e) PDMS peeling off the mold, and (f) Fully non-planar PDMS chip.

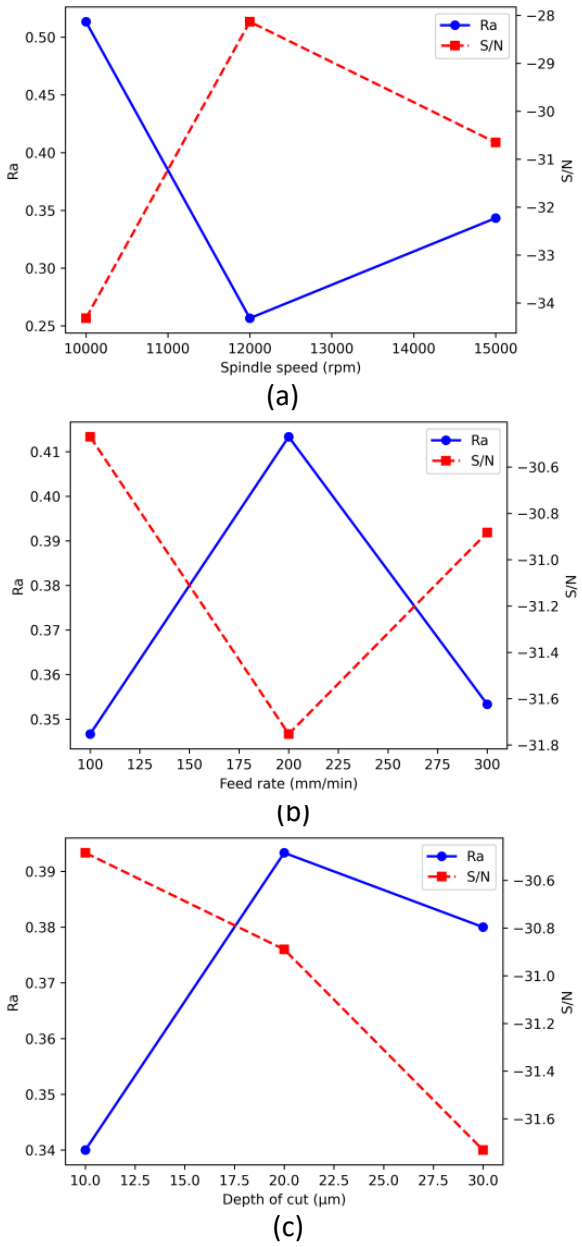

Figure 4. S/N ratios and surface roughness corresponding to three main factors and three levels: (a) Spindle speed, (b) Feed rate, and (c) Depth of cut.

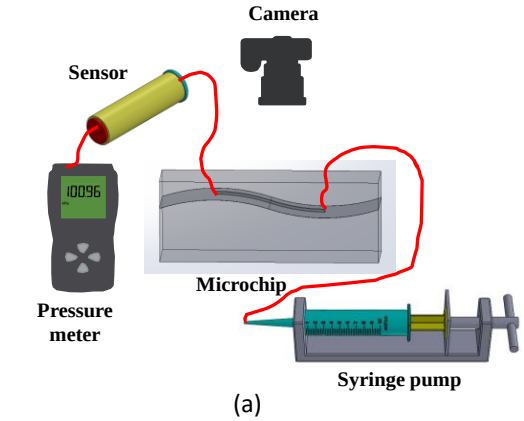

(a)

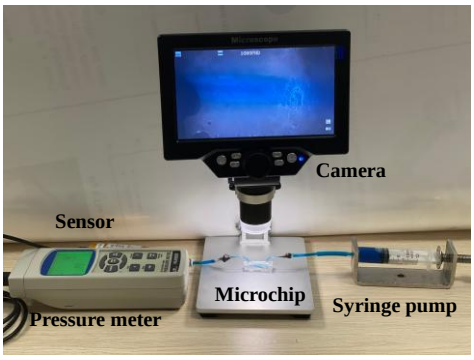

(b)

Figure 5. (a) System used to test the bonding strength of bonded microfluidic chips, including a camera, , a pressure meter, a manual syringe pump with a pressure sensor, and (b) Experiment setup.

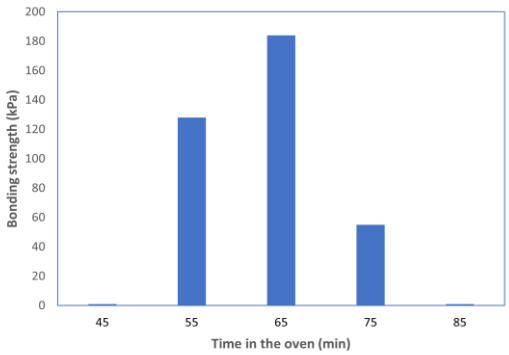

Figure 6. The bonding strength of the PDMS chip as a function of the partial-curing time at 65 °C

Table 4. Ball-end mill specifications, toolpath strategy, and machining conditions.

Parameter	Value
Type	Ball-end mill
Material	Carbide Micro Grain
Diameter	Radius-0.5 mm
Stepover	0.1mm
Cut pattern	Zig Zag
Drive Method	Surface Area
Cooling	Air

Table 5. Experimental results based on various factors and levels

No.	(A)-Spindle speed (r.p.m)	(B)-Feedrate (mm/min)	(C)- DOC (µm)	Ra (µm)
1	10,000	100	10	0.42
2	10,000	200	20	0.69
3	10,000	300	30	0.35
4	12,000	100	20	0.21
5	12,000	200	30	0.27
6	12,000	300	10	0.29
7	15,000	100	30	0.41
8	15,000	200	10	0.31
9	15,000	300	20	0.34

Table 6. Factor to analysis cutting parameter

Level	(A)-Spindle speed (r.p.m)	(B)-Feedrate (mm/min)	(C)-DOC (µm)
1	6.533	9.480	9.350
2	11.763	8.230	8.630
3	9.033	9.620	9.350
Max	11.763	9.620	9.350
Min	6.533	8.230	8.630
Range	5.230	1.390	0.720
Rank	1	2	3